Highly loaded UV curable nanosilica dispersions for rapid prototyping applications

Maciej Wozniak [a,b,*], Thomas Graule [a], Yoram de Hazan [a], Dariusz Kata [b], Jerzy Lis [b]

[a] *Empa, Swiss Federal Laboratories for Materials Testing and Research, Laboratory for High Performance Ceramics, Überlandstrasse 129, CH-8600 Dübendorf, Switzerland*
[b] *University of Science and Technology, Department of Technology of Ceramics and Refractories, Al. Mickiewicza 30, 30-059 Krakow, Poland*

Abstract

Silica microcomponents are attractive for applications requiring high temperature stability and chemical durability such as in microreactors. Rapid prototyping methods of forming ceramic dispersions hold great potential for manufacturing of microreactors. Stereolithography for example can benefit from highly solid loaded, low viscosity and high transparency dispersions. This article presents the development of >40 vol.%, UV curable transparent silica nanodispersions having viscosities suitable for stereolithography applications. The main parameters enabling these high loading dispersions are minimization of the Van der Waals attractive forces and affinity of monomer end group for the silica surface (e.g. hydrogen bonding). The minimization of the Van der Waals attraction is achieved by refractive index matching of the nanosilica and UV curable acrylate monomers. This results also in highly transparent dispersions having curing depths in the order of 10 mm in the UVA range. The transformation of selected dispersions to self-supporting silica glass sheets through UV curing, debinding and sintering was investigated by TGA/DTA, dilatometry and XRD.
© 2009 Elsevier Ltd. All rights reserved.

Keywords: A. Stereolithography; B. Nanosilica; C. Microreactors; D. UV curing; E. Glass; F. Nanodispersion

1. Introduction

A great challenge in advanced processing of ceramic microtechnology is the manufacture of a new class of microreactors working both at room and elevated temperatures.[1] On the market are already available microreactors made from glass, silicon, stainless steel, metals and polymers.[2] Application of microreactors made from polymers is limited due to their low thermal stability and from metals because of relatively low chemical stability of metallic alloys. Therefore ceramics and special corrosion resistant glasses and pure silica glass, as chemically inert materials, are much more suitable for building efficient microreactors having long-term use at high temperatures. Glass as transparent material can be useful also for photochemical reactors or for cases where visual inspection of reactions is important.

Development of microshaping techniques is an important factor determining the progress of microtechnology. Therefore during last decade the importance of LIGA processing, soft and hard micromachining, screen printing (SC) and rapid prototyping (RP) has grown rapidly.[3] The major advantage of RP is the possibility to shape 3D objects designed by computer and produced as hardware by laser or by UV lamp irradiation. These technologies allow microreactor components of micrometer dimensions to be prepared within a short time and with a pattern resolution up to 1 μm.[4] Therefore they are very convenient for manufacturing of prototypes for further testing. High loading, high transparency ceramic dispersions in UV curable vehicle are desirable for development of ceramic microtechnology. In stereolithography where the objects are built out of thin layers, high UV transparency is not a prerequisit. At the same time, the reduced scattering is advantageous for high resolution lithography.

Previous papers concerning ceramic dispersions in UV curable non-polar resins and their uses for stereolithography are known. For example in Ref. [5] authors present curing of dispersions containing alumina and zircon, other include PZT in Ref. [6], BaTiO$_3$[7] or micrometer size silica.[8] These form the base

* Corresponding author at: University of Science and Technology, Department of Technology of Ceramics and Refractories, Al. Mickiewicza 30, 30-059 Krakow, Poland. Tel.: +48 502 138 738.
E-mail address: wozniak@agh.edu.pl (M. Wozniak).

of our research which pertains to the possibility of nanosilica dispersions in acrylates and their UV curability.

Ceramic bodies produced from nanoparticles frequently show excellent sintering behavior[4,9,10] and provide sufficient resolution for the fine microstructures.[11] Furthermore nanoparticles can reduce UV light scattering in the highly particle loaded resin. Scattering processes significantly reduce the intrusion depth of UV radiation into the slurry and therefore reduce the maximum cured thickness of the resin.

Rheological properties of nanodispersions strongly depend on both the particle–particle and particle–solvent interactions in systems that influence dispersion stability. There are many factors which can affect these interactions, including liquid phase viscosity, pH, ionic strength, particle size, particle volume fraction, specific surface area and the presence of soluble polymers or surfactants.[12] In order to optimize a nanodispersed system, suitable for stereolithography applications, rheological behavior must be controlled.[13] The stability of the dispersion is crucial and can change the rheology dramatically. For example, when a nanodispersion becomes colloidally unstable, the viscosity can increase by several orders of magnitude and yield stress can develop.[14]

Colloid stability and therefore rheological behavior of ceramic pastes can be described by the DLVO theory (named after Derjaguin, Landau, Verwey and Overbeek), according to which total energy between two colloidal particles is given by the following equation[15,16]:

$$V_{Total} = V_{vdW} + V_{elect} + V_{steric} \qquad (1)$$

where V_{vdW} (Van der Waals) is an attractive interaction, $V_{elect} + V_{steric}$ are mainly repulsive interactions.

In the non-aqueous dispersions investigated in this study electrostatic forces contribution is very small. Introduction of steric barriers between particles and dispersing medium is another way to induce colloidal stability. This can be done for example by adsorption of polyelectrolyte surfactant on the particle which keeps them in distance beyond the Van der Waals attraction force reach their flocculation.[17,18]

However, the large variety of UV curable monomers provides an alternative route for high loaded colloidal dispersions. Properties of dispersing medium can play a meaningful role in reduction of particle–particle Van der Waals attraction. The Van der Waals attraction for two identical spheres of radius a separated by a distance h can be expressed by the effective Hamaker constant (A):

$$V_{vdW} = \frac{-Aa}{6\pi h} \quad (h \ll a) \qquad (2)$$

The effective Hamaker constant is given by

$$A = a\left(\frac{\varepsilon_m - \varepsilon_p}{\varepsilon_m + \varepsilon_p}\right)^2 + b\frac{(n^2 - n^2)^2}{(n^2 + n^2)^{3/2}} \qquad (3)$$

where ε is the dielectric constant, n is the refractive index and a and b are constants.[19] The subindices m and p refer to the dispersing medium and the dispersed particles, respectively. When the refractive indices of the interacting media are matched, i.e.

when $n_p = n_m$, the second term in Eq. (3) vanishes. The dielectric constant depends on the complex refractive index through Eq. (4). The first term in Eq. (3) may also become negligible when both the real and imaginary parts of the complex refractive indices (n_C) are matched,

$$\varepsilon = n_C{}^2 \qquad (4)$$

Thus it follows that the selection of dispersing medium having refractive index matched to the dispersed phase can result in highly loaded dispersions due to minimization of the Van der Waals attraction forces.[19]

This approach for dispersion stabilization of UV curable systems is furthermore highly beneficial since the transparency of such dispersion is expected to be superior compared to non-refractive index matched systems.[13] This index matching may enable efficient curing of thick layers.[20]

The hydrophilic silica colloids are used as a thickening agent for low polar media which do not have ability to initiate hydrogen bonding.[21] This is due to flocculation of the silica particles and is undesirable in preparation of high loaded dispersions. This means that in addition to refractive index matching the polarity of monomers with hydrogen bonding capability (or other favourable surface interactions) also play a significant role in dispersion stability.

In this paper we present the development of highly loaded nanosilica dispersions in UV curable mixtures of monomers enabled by selection of monomers with matched refractive index and polarity. The transformation of selected nanodispersions to self-supporting silica glass sheets through UV curing, debinding and sintering are presented.

2. Experimental

2.1. Materials

Commercially available SiO$_2$ nanopowder, Aerosil OX50, was purchased from Evonik, Germany. The OX50 specific surface area measured with ASAP 2010 Micromeritics (USA) is 54 m^2/g. A TEM picture of this SiO$_2$ nanopowder used in this study is shown in Fig. 1. The particles have spherical shape, and their size is in the range of 40–80 nm. Tables 1 and 2 show the monomers and photoinitiators used in this study. Five types of monomers were tested as potential dispersing media for OX50 (4HBA, HEA, butyl acrylate, M200 and M282-PEGDA). Three photoinitiators (Genomer ITX, Genocure TPO and Genocure LTM) were used for initiation of UV curing.

All monomers were selected since they have refractive indices close to silica in order to reduce the Van der Waals attraction. Additional benefit is the transparency of the slurries. The difunctional M200 and PEGDA promote high crosslinking density of the polymeric matrix beneficial for the strength of the cured samples, but have relatively non-polar end groups. In contrast 4HBA and HEA are monofunctional and are terminated with a polar OH group. The methyl terminated butyl acrylate is a non-polar analog of 4HBA and HEA and provides direct
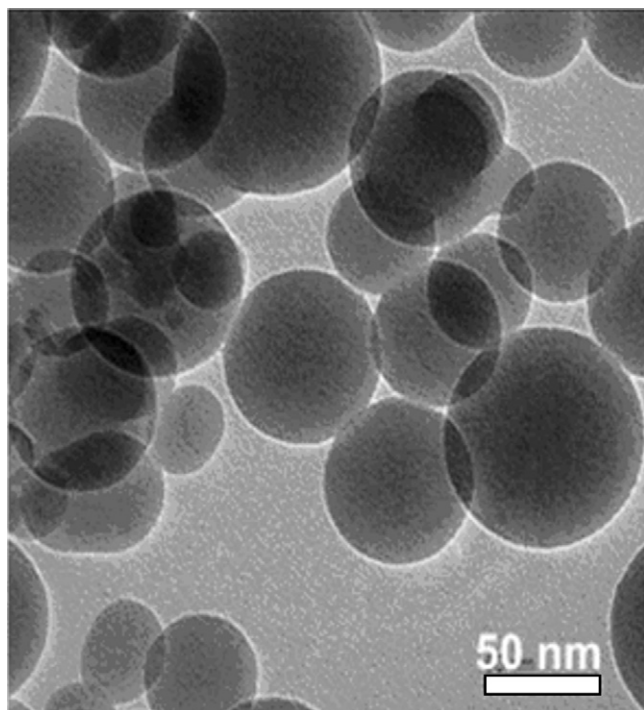
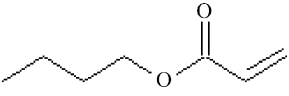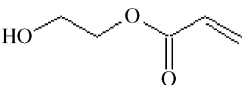## 2.2. Dispersion preparation and characterization
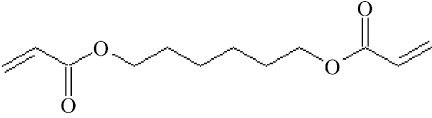
In order to prepare nanosilica dispersions in mixture of monomers a laboratory dissolver, Ultra Turrax T 50 (USA), was used. Dispersions containing 10–40 vol.% of nanosilica in different monomer mixtures were made. The rheological behavior of the pastes was tested at 23 °C with a rotational viscosimeter (Rheolab MC120, Physica Messtechnik GmbH, Germany) with a volume of 3 cm^3 and a gap of 0.59 mm between the two cylinders. The viscosity of the dispersions was measured for shear rate of 100 s^{-1} repeating three times to ensure good reproducibility. The viscosity as a function of shear rate was also measured up to 1000 s^{-1}.

The UV transmission spectra of pure monomer mixtures and silica dispersions in these mixtures were measured by Cary 50 UV–Vis spectrophotometer (USA) between 200 and 800 nm. The specimen thickness was 1 cm.

2.3. Molding and UV curing

Shortly before molding, 5% of photoinitiator (based on monomer mixture) was added to the dispersion. The dispersions were cast in a 10 cm × 10 cm Teflon mold having a depth of 1 mm and were subsequently cured in a curing chamber for 15–40 s. Due to the high transparency of the system it was possible to cure 1 cm thick samples for dilatometry in a similar fashion. A curing chamber Uvacube100 (Hönle, UV Technology, Switzerland) was used with an iron bulb producing a UV spectrum which is the most intense in the UVA range and power of 100 W.

Fig. 1. TEM micrograph of nanosilica OX50.

comparison of the effect of end group polarity on dispersion quality. Despite of possibly remaining sulfur or phosphorus containing residues the photoinitiators were chosen because of their UV absorption range which is compatible with monomers and UV irradiation source.

Table 1
Raw materials used for the preparation of nanosilica UV curable dispersions.

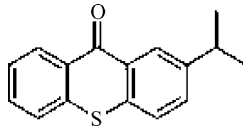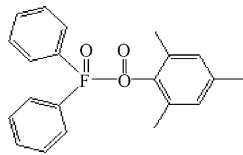| Name, provider	Function	Formula	n	Density
Aerosil OX50, Evonik, D	Glass former	Amorphous SiO$_2$	1.460	2.2 g/cm^3
M200[a], Rahn, CH	Monomer		1.456	1.03 g/cm^3
Butyl acrylate, Sigma, USA	Monomer		1.417–1.419	0.898 g/cm^3
4HBA[b], BASF, D	Monomer		1.454	1.039 g/cm^3
HEA[c], BASF, D	Monomer		1.451–1.454	1.106 g/cm^3
M282[d], Rahn, CH	Monomer		1.464	1.12 g/ml

[a] 1,6-Hexanediol diacrylate.
[b] 4-Hydroxybutylacrylate.
[c] 2-Hydroxyethyl acrylate.
[d] Polyethyleneglycol 200 diacrylate.

Table 2
List of photoinitiators used to curing silica dispersions.

Name, provider	Function	Formula	Absorption range
Genomer ITX[a], Rahn, CH	Photoinitiator		259–383 nm
Genocure TPO[b], Rahn, CH	Photoinitiator		253–368 nm
Genocure LTM, Rahn, CH	Photoinitiator	<25% of Genocure TPO	380 nm

[a] Thioxanthone.
[b] 2,4,6-Trimethylbenzoyldiphenylphosphine oxide.

2.4. Debinding and sintering

Debinding and sintering behavior was analyzed by dilatometry using DIL 802 Bähr-Thermoanalyse GmbH, Germany and TG/DTA using STA 409 C/CD, Netzsch, Germany. The analysis in both cases consisted of heating up to 1250 °C at 10 °C/min. The samples were debinded and sintered with the optimized temperature profile shown in Table 3.

After sintering samples were examined by XRD (X'Pert Pro, Panalytical, The Netherlands) to assess crystalline phases.

3. Results and discussion

In this study we used refractive index matching of the dispersive liquid and dispersed phase as means to decrease the particle–particle attraction forces. This is particularly important to enable high solid loading nanodispersions having low viscosity suitable for stereolithography applications. UV curable monomers with matched refractive indices to silica were selected as the dispersive phase (Table 1). However, refractive index matching alone is not a sufficient criterion for high solid loading dispersions. For example, using the refractive index matched, difunctional polyethyleneglycol 200 diacrylate (PEGDA) or 1,6-hexanediol diacrylate (Miramer M200) resulted in viscous dispersions exceeding the maximum viscosity limit for stereolithography applications (5 Pa s at 30 s^{-1})[22] with only 15–18 vol.% nanosilica. Even the usage of the highly innovative microstereolithography apparatus, designed by EPFL, which allows curing of dispersion with viscosities up to 10 Pa s for 100 s^{-1} in 26 °C[23] is debatable. In order to obtain highly loaded dispersions the hydrophobic/hydrophilic interactions of the dispersion medium and the dispersion phase need also to be considered. Due to that the monofucnctional 4HBA and HEA which are OH terminated (see Table 1) were chosen for further experiments. These monomers are able to form hydrogen bonding with the hydroxyl groups present on the silica surface and thereby increase the surface compatibility to the monomer. 40 vol.% of nanosilica dispersions with suitable viscosities were obtained using these monomers.

However, using only monofunctional UV curable monomers results after UV curing in elastic sheets of low durability. A high crosslinking density can be achieved with the use of multifunctional monomer. In order to produce sheets with good mechanical properties while maintaining acceptable dispersion viscosity, a monomer mixture containing monoacrylate (4HBA or HEA) and 7 vol.% of the difunctional acrylate PEGDA was found optimal. The viscosity (measured at shear rate of 100 s^{-1}) as a function of nanosilica content in these monomer mixtures are shown in Fig. 2. Viscosity increases with concentration of silica in both cases but the rate of increase with HEA is significantly lower. The viscosity of 4HBA and HEA based dispersions for 40 vol.% nanosilica is 1.75 and 0.5 Pa s, respectively: both values are below maximum viscosity limit for stereolithography. In contrast, only 10 vol.% of nanosilica could be dispersed in butyl acrylate before approaching the maximum acceptable value of viscosity for stereolithography.
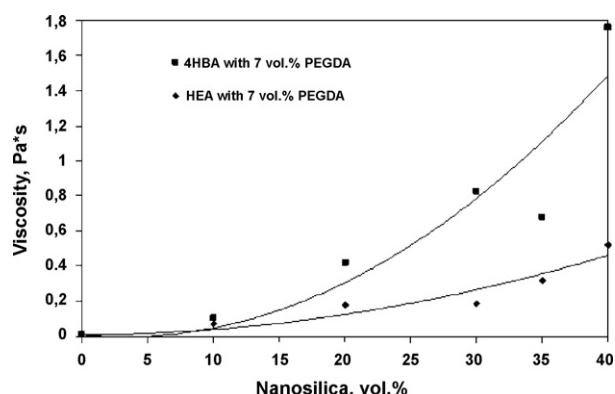
Table 3
Debinding and sintering program.

Segment	1	2	3	4	5	6
Ramp (K/h)	60	–	150	–	300	–
Temperature (°C)	500	500	750	750	1250	1250
Holding time (h)	None	2	None	2	None	2 end

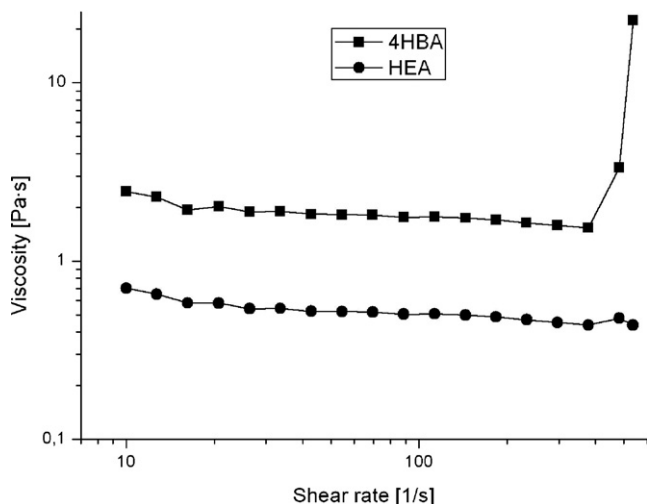Fig. 2. Influence of the monomer mixture on the viscosity (measured at 100 s^{-1}).

Fig. 3. 40 vol.% nanosilica OX50 4HBAwith 7 vol.% PEGDA and 40 vol.% nanosilica OX50 HEA with 7 vol.% PEGDA.

The above findings indicate that the increased polarity induced by either end group modification (OH vs. CH₃ or acrylate) or hydrocarbon spacer shortening (HEA vs. 4HBA) can dramatically improve dispersion.

Up to the maximal shear rate for stereolithography (100 1/s) (Fig. 3) all dispersions are shear thinned or behave like Newtonian liquids. For values between 400 and 800 1/s, respectively to the sample a sudden increase in shear stress is observed. These results potentially suggest that the hydrogen bridges enabling high loading dispersions are broken under high shear conditions. This paper will not elaborate on the subject.

Fig. 4 presents the transmission spectra of momomers mixture and nanosilica dispersion in the UV–vis range. Both particle free monomer mixtures (HEA with 7% PEGDA and 4HBA with 7% PEGDA) are >90% transparent down to 320 and 380 nm, respectively. Below this wavelength the transmission of both monomer mixtures is decreased rapidly. No transmittance exists below 310 nm. The transmission of the 20 vol.% nanosilica dispersions in these monomer mixtures in the UVA is only 5–20% lower than that of the pure monomer mixtures. The silica dispersion in the HEA mixture loses transparency at somewhat longer wavelengths. The silica dispersions exhibit a broad and shallow valley in transmission spectra between 400 and 600 nm. This phenomenon is not currently understood and requires additional investigation.
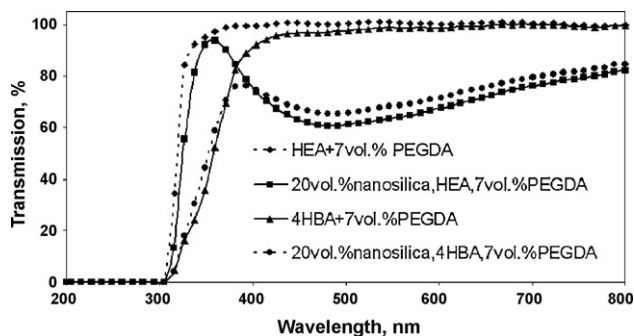

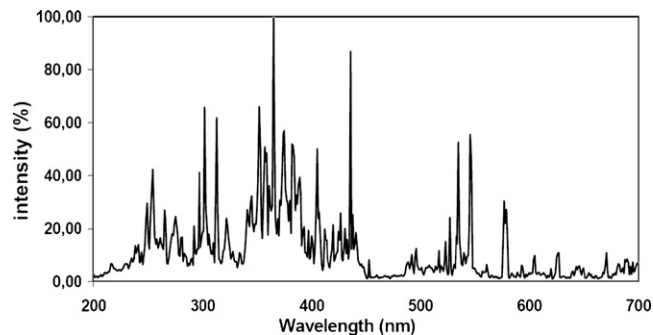Fig. 4. UV–vis spectra of silica nanodispersions and pure mixture of monomers.

Fig. 5. UV spectra of UV lamp (Hönle, Switzerland).

3.1. Curing, debinding and sintering

The photoinitiators Genocure ITX, LTM and TPO were chosen because their UV absorption range is compatible with that of the silica nanodispersions and UV spectrum of the Fe curing lamp (see Table 2) and Fig. 5.

Samples containing up to 40 vol.% of silica and 5% photoinitiator in HEA/PEGDA and 4HBA/PEGDA mixtures were cast in a 10 cm × 10 cm Teflon mold having a depth of 1 mm and cured in a curing chamber. Curing time for samples containing HEA was 15–25 s and was shorter than for those with 4HBA, which was up to 40 s. Both sheets from HEA and 4HBA with nanosilica dispersions experienced slight warpages caused by surface tensions.

It is also found that the use of TPO and LTM (containing <25% TPO) photoinitiators lead to sheets with good mechanical properties whereas the use of ITX lead to weak and brittle samples after curing and sintering.

Figs. 6 and 7 present the dilatometry and TG/DTA results in the 25–1250 °C temperature range, respectively, for a UV cured sample having 40 vol.% nanosilica in 4HBA/PEGDA. As shown in Fig. 6, samples show an expansion of 1–2% up to 300 °C. This is likely caused by the relatively high thermal expansion coefficient of the polymer matrix. The TGA shows three steps of weight loss: (i) 10% weight loss accompanies the expansion seen by dilatometry during the first step of polymer decomposition, (ii) the second and major decomposition step results in weight loss of ∼25% between 250–450 °C (Fig. 7). This corresponds
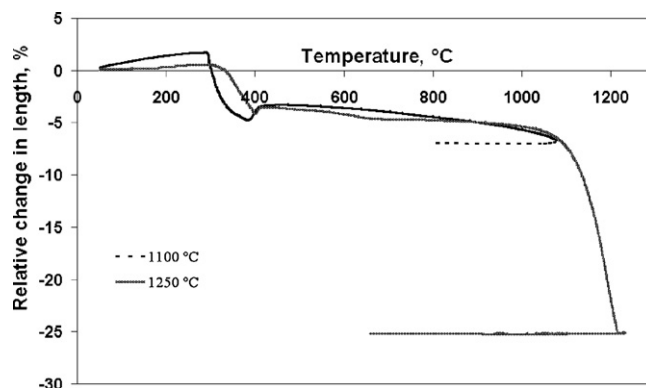

Fig. 6. Dilatometry measurement of 40 vol.% nanosilica with 4HBA/PEGDA dispersion with TPO photoinitiator.
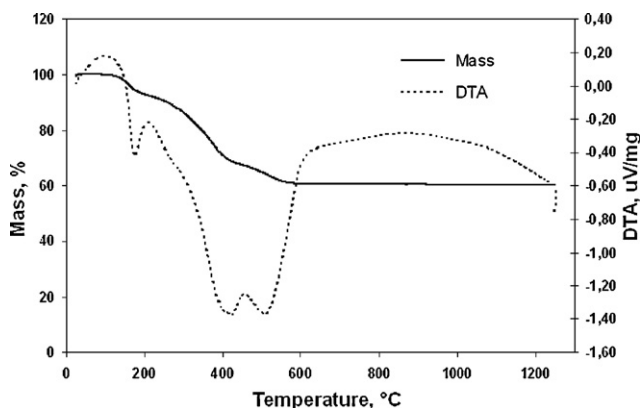
Fig. 7. TG-DTA 40 vol.% nanosilica (4HBA/PEGDA and 5% TPO).

Fig. 9. Results of XRD from sintered sheets made with addition of different (5%) photoinitiators.

to ~7% shrinkage detected by the dilatometer, and (iii) the third weight loss step terminates at 570 °C. Above 570 °C no further weight loss is observed. The total weight loss of 40.5% found by TGA is in good agreement with the expected 42% according to the recipe. A gradual shrinkage is observed in Fig. 6 at temperatures between 550 and 1150 °C. The sample heated to 1100 °C shows very little sintering (7% shrinkage) while the one at 1250 °C end up with 25% total linear shrinkage. This corresponds to ~37–38 vol.% initial silica content in good agreement with the expected 38 vol.% (after photoinitiator addition).

The debinding temperature of 500 °C and sintering temperature 1250 °C (Table 3) were selected based on the TGA and dilatometry results above. The measured density of the sample treated in 1250 °C is 2.17 g/cm^3, this is close to the theoretical value of amorphous silica which is 2.20 g/cm^3, therefore such a sample is sintered to ≈99% density.

Fig. 8 shows examples of sintered sheets based on samples having 40 vol.% nanosilica in 4HBA (14:1 M282) monomer mixture and different photoinitiators. Sheets with thickness of ~0.6 mm cured using Genocure LTM and ITX photoinitiators are transparent whereas the sheet cured with Genocure TPO is white and translucent. Fig. 9 shows XRD results of the samples
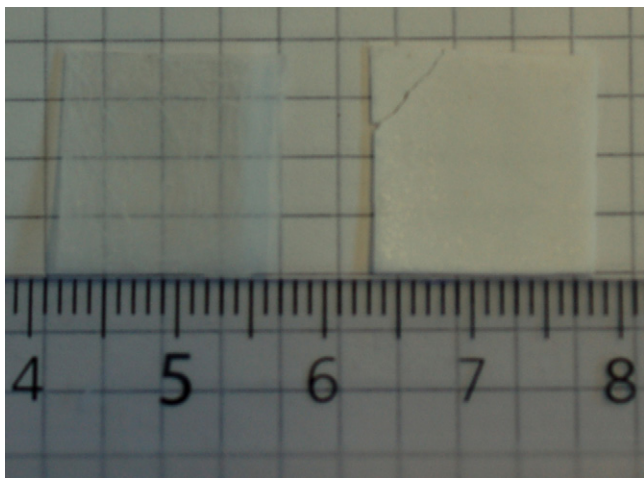
presented in Fig. 8. The ITX and LTM based samples are amorphous whereas the TPO based sample consists mainly of a low temperature cristobalite phase. The crystallization in the case of TPO may be related to the presence of high level of phosphorus in the photoinitiator. Lower amount (<25%) of phosphorus as in the case of LTM does not lead to crystallization in this system. Based on these results future activities will concentrate on shaping complex, transparent silica parts by stereolithography.

4. Summary

Nanosilica dispersions suitable for stereolithography applications were developed. The dispersions exhibit low viscosity (0.5–1.8 Pa s) at 100 s^{-1} and high transparency at solid loadings of 40 vol.%. This is enabled by a proper selection of monomers having matched refractive index and hydrophilic properties to silica. The use of >5% TPO photoinitiator leads to mechanically robust but crystalline sheets after sintering. The use of 5% ITX photoinitiator results in transparent silica glass having poor mechanical stability. And finally, the use of 5% LTM photoinitiator leads to both transparent silica glass and acceptable mechanical stability.

Fig. 8. Examples of sintered sheets with different photoinitiators, left—sample made with 5% LTM photoinitiator; right—sample made with 5% TPO photoinitiator.
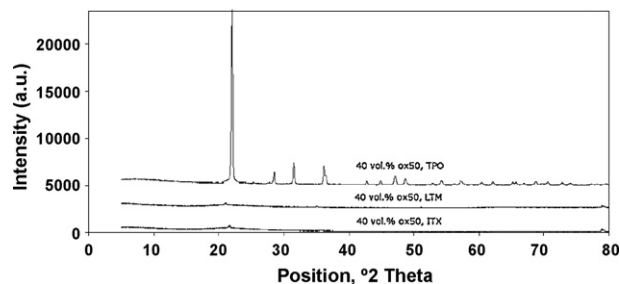
References

1. Jensen, K. F., Microreaction engineering—is small better? *Chemical Engineering Science*, 2001, **56**, 293–303.
2. Seeberger, P. H., Microreactors as the key to the chemistry laboratory of the future. In *IUPAC/OPCW international workshop the impact of advances in science and technology on the chemical weapons convention*, 2007.
3. Hessel, V., Hardt, S. and Löwe, H., *Chemical micro process engineering*. Wiley–VCH Verlag GmbH & Co., KGaA, 2004.
4. Pampuch, R., New materials and technologies. *Bulletin of the Polish Academy of Sciences, Technical Sciences*, 2004, **52**(4).
5. Delmotte, C., Erauw, J. P. and Cambier, F., Manufacturing of complex ceramic parts by selective curing of pastes. *Key Engineering Materials*, 2004, **264–268**, 701–706.
6. Defaud, O., Marchal, P. and Corbel, S., Rheological properties of PZT suspensions for stereolithography. *Journal of the European Ceramic Society*, 2002, **22**, 2081–2092.

7. Jang, J. H., Wang, S., Pilgrim, S. M., Schulze, W. A. and Preparation, Characterization of barium titanate suspensions for stereolithography. *Journal of the American Ceramic Society*, 2000, **83**(7), 1804–1806.

8. Esposito, C., Corcione, A., Greco, A., Montagna, F., Licciulli, A. and Maffezoli, A., Silica moulds built by stereolithography. *Journal of Materials Science*, 2005, **40**, 4899–4904.

9. Clasen, R., High-purity glasses and ceramics prepared by sintering compacts of nanosized particles: advantages and perspectives. *Euro Ceramics*, 2002, **VII**(Pt 1–3), 235–238.

10. Heiber, J., Clemens, F., Graule, T. and Hülsenberg, D., Fabrication of silica glass fibers by thermoplastic extrusion. *Glass Science and Technology*, 2004, **77**, 211–216.

11. Schönholzer, U., Hummel, R. and Gauckler, L. J., Microfabrication of ceramics by filling of photoresist molds. *Advanced Materials*, 2000, **12**(17), 1261–1263.

12. Bergström, L., Surface chemical characterization of ceramic powders. In *Surface and colloid chemistry in advanced ceramics processing*, ed. R. J. Pughs and L. Bergström. *Surfactant science series*, *vol. 51*. M. Dekker Inc., 1994, pp. 71–125.

13. Chartier, T., Chaput, C., Doreau, F. and Loiseau, M., Stereolithography of structural complex ceramic parts. *Journal of Materials Science*, 2002, **37**, 3141–3147.

14. Hidber, P., Graule, T. J. and Gauckler, L. J., Influence of the dispersant structure on properties of electrostatically stabilized aqueous alumina suspensions. *Journal of the European Ceramic Society*, 1997, **17**, 239–249.

15. Lewis, J. A., Colloidal processing of ceramics. *Journal of American Ceramic Society*, 2000, **83**(10), 2341–2359.

16. Everett, D. H., *Basic principles of colloid science*. Royal Society of Chemistry, 1988.

17. De Hazan, Y., Reuter, T., Werner, D., Clasen, R. and Graule, T., Interactions and dispersion stability of aluminum oxide colloidal particles in electroless nickel solutions in the presence of comb polyelectrolytes. *Journal of Colloid and Interface Science*, 2008, **323**, 293–300.

18. Zürcher, S. and Graule, T., Influence of dispersant structure on the rheological properties of highly-concentrated zirconia dispersions. *Journal of the European Ceramic Society*, 2005, **25**, 863–873.

19. Kizling, J., Kronberg, B. T. and Eriksson, J. C., On the formation and stability of high internal phase O/W emulsions. *Advances in Colloid and Interface Science*, 2006, **123–126**, 295–302.

20. Cui, M. M. and Adrian, R. J., Refractive index matching and marking methods for highly concentrated solid–liquid flows. *Experiments in Fluids*, 1997, **22**, 261–264.

21. Raghavan, S. R., Walls, H. J. and Khan, S. A., Rheology of silica dispersions in organic liquids: new evidence for solvation forces dictated by hydrogen bonding. *Langmuir*, 2000, **16**, 7920–7930.

22. Licciulli, A., Esposito Corcione, C., Greco, A., Amicarelli, V. and Maffezzoli, A., Laser stereolithography of ZrO_2 toughened Al_2O_3. *Journal of the European Ceramic Society*, 2005, **25**, 1581–1589.

23. Bertsch, A., Jiguet, S. and Renaud, P., Microfabrication of ceramic components by microstereolithography. *Journal of Micromechanics and Microengineering*, 2004, **14**, 197–203.